Paper presented at the Ninth Symposium on Engineering Problems of Fusion Research, Chicago, Illinois, October 26-29, 1981; also for publication in the Proceedings.

INTOR RADIATION SHIELDING FOR PERSONNEL ACCESS*

Y. Gohar and M. Abdou

Argonne National Laboratory
Argonne, Illinois 60439

*Work supported by the U. S. Department of Energy.

INTOR RADIATION SHIELDING FOR PERSONNEL ACCESS*

Y. Gohar and M. Abdou

Argonne National Laboratory
Argonne, Illinois 60439

Summary

The INTOR radiation shield system was designed to satisfy the design constraints and perform several functions. The main function during reactor operation is to provide sufficeint neutron and photon attenuation to (a) protect the different reactor components from radiation dmage and nuclear heating; (b) reduce the induced activation level in reactor components; and (c) protect the plant worker and the public from radiation exposure. Another requirement that was a major factor in the INTOR shield design is to permit personnel access to the reactor hall, with all shield in place, within 24 h after shutdown which significantly reduces the reactor downtime for maintenance. In order to satisfy the dose requirements, the design was carried out in two steps: (a) the outboard bulk shield (without penetrations) was optimized to achieve $\leq$2.5 mrem/h within a day after shutdown; and (b) the penetration shields for the neutral beams and divertor were designed to keep the total exposure dose $\leq$2.5 mrem/h. Since penetration shield significantly affects reactor cost, personnel access, and reactor availability, elaborate three-dimensional radiation calculations for the whole reactor system, including the neutral beams, divertor system, toroidal field coils, and reactor building liner, were carried out. The general-purpose Monte Carlo code MCNP was used for the calculations with a continuous energy representation for the nuclear cross section from ENDF/B-IV. The energy and spatial distributions of the D-T plasma source neutrons were modeled in the calculations. A coupled neutron and neutron-induced photon transport during the reactor operation and decay gamma transport after shutdown were performed. The results show the following shield thicknesses required to provide personnel access: (a) 100-cm bulk shield behind a 50-cm tritium breeding blanket; (b) 100 cm for neutral beam drift tubes; (c) 75 cm for surfaces of the beam injector box facing the drift tubes; (d) 50 cm for the rest of the neutral beam system and divertor ducts.

Introduction

The INTOR reactor shield system[1] consists of the blanket, bulk shield, penetration shield, component shield, and biological shield. The bulk shield consists of two parts: (a) the inboard shield; and (b) the outboard shield. The distinction between the different components of the shield system is essential to satisfy the different design constraints and achieve various objectives.

Inboard Blanket and Shield

The inboard blanket and shield was designed to protect the toroidal field (TF) coils using Type 316 stainless steel, Fe-1422, B_4C, and H_2O as shielding materials. The inboard blanket serves only the shielding function and does not produce tritium. The total available radial thickness for the inboard blanket and shield is 0.78 m since a portion of the inboard Δ^i_{BS} is used for other functions (15-cm steel jackets for the TF coils; 17-cm vacuum gaps for thermal expansion, thermal insulation, and engineering tolerance). In the backup design of carbon armor for the inboard first-wall protection, the available radial thickness drops to 0.73 m to allow 0.05 m for the armor.

*Work supported by U. S. Department of Energy.

An optimization process was performed to define the composition of the inboard shield using a homogeneous mixture model with Fe-1422, H_2O, and B_4C materials. The results from the homogeneous model were used as input for a heterogeneous analysis to account for the engineering considerations and benefits from redistribution of the shielding material to get more protection for the TF coils.

An extensive analysis based on a one-dimensional cylindrical model was performed to define the optimum homogeneous composition of the shield. Table 1 lists the blanket and shield parameters used in the calculations and Fig. 1 shows a schematic of the geometry considered. The calculations were performed for a wide range of compositions for the inboard blanket and shield region. The volume fraction of Fe-1422 was varied from 0.1 to 0.9 for the four different B_4C volume fractions; 0, 0.1, 0.3, and 0.5 with the balance as H_2O. A sample of the results is given in Fig. 2 for the nuclear heating in the TF coils as a function of the Fe-1422 volume fraction for the four boron carbide volume fractions with the balance being H_2O.

Table 1. Dimensions and Material Compositions of the INTOR Inboard Blanket, Shield, and TF Coils Used in the One-Dimensional Homogeneous Model

Component	Major Radius (cm) From	To	Density Factor	Composition Volume Percentage
TF case	190	200	1.0	100% 316 SS
TF superconductor	200	270	1.0	2.6% Nb_3Sn
			1.0	24% Cu
			1.0	37.7% 316 SS
			1.0	28.5% He
			1.0	7.2% epoxy
TF case	270	280	1.0	100% 316 SS
Thermal insulator	280	290	0.01	100% epoxy
TF dewar	290	295	1.0	100% 316 SS
Vacuum gap	295	299	0.0	Vacuum
Shield	299	374	1.0	x% Fe-1422
			0.9	y% B_4C
			1.0	(100-x-y)% H_2O
First wall	374	375	1.0	50% 316 SS 50% H_2O
First wall armor	375	390	1.0	100% C

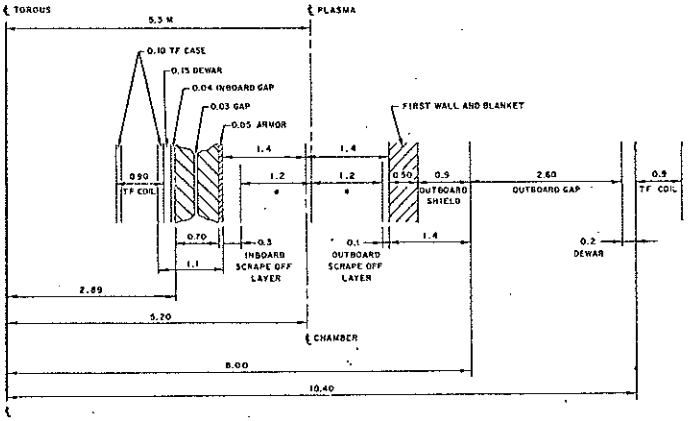

Fig. 1. Midplane INTOR geometry for shielding analysis.

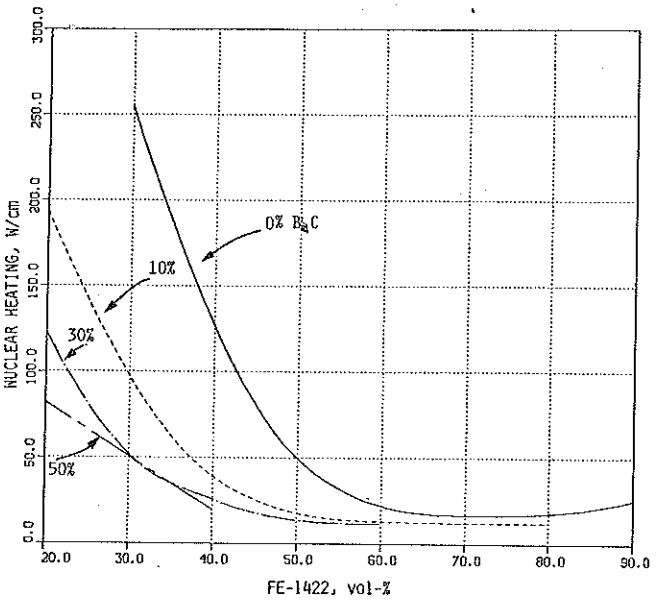

Fig. 2. Nuclear heating in the TF coils (including magnet case and magnet dewar) per cm of the magnet height for 1.3 MW/m^2 neutron wall loading as a function of the Fe-1422 concentration in the inboard blanket and shield for different boron-carbide concentrations (balance is H_2O).

Figure 3 shows the maximum nuclear heating in the superconductor, the magnet case, and the magnet dewar per cm of the magnet length (circumference of the D-shape). Both the nuclear heating in the TF coils and the maximum nuclear heating in the TF case show a minimum at the same blanket and shield composition. The total nuclear heating in the TF coils based on the results in Fig. 3 is less than the 5-kW design limit for the TF coils. The maximum dose after 6 $MW-y/m^2$ neutron wall exposure in the thermal insulator shows a resemblance to the nuclear heating in the TF coils shown in Fig. 3. The neutron dose accounts for more than 75% of the total dose except for the blanket and shield compositions without B_4C. The gamma dose in the insulator materials is higher for lower B_4C percentage because of the increase in the gamma flux caused by radiative capture of the low energy neutrons in the Fe-1422 material. The maximum doses in the thermal and electrical insulators have minimum values of 2.8×10^9 and 8.8×10^8 rad, respectively at 80% Fe-1422, 10% B_4C, and 10% H_2O composition, where the design limit for the damage in the insulators is 10^{10} rad. The neutron fluence (E > 0.1 MeV) in the superconductor after 6 $MW-y/m^2$ neutron exposure shows the lowest values in the range of 70-80% Fe-1422 concentration. The minimum neutron fluence is $\sim 5 \times 10^{17}$ n/cm^2 at the end of life which is less than the threshold for the radiation damage in the Nb_3Sn superconductor. The maximum induced resistivity and atomic displacement per atom (dpa) have minimum values of 4.3×10^{-8} Ω-cm and 3.4×10^{-4} dpa respectively, for a blanket and shield composition of 80% Fe-1422, 10% B_4C, and 10% H_2O. From the above results, it appears that a composition of 80% Fe-1422, 10% B_4C, and 10% H_2O is an optimum choice for the magnet protection based on the homogeneous composition analysis.

Practical considerations dictate a heterogeneous arrangement for the inboard blanket and shield. Possible heterogeneous arrangements were analyzed to maximize the magnet protection. The inboard blanket and shield consists of two parts. The first part is integrated with the removable torus sector module. The second part is a semi-permanent shield. The radial thickness of the first part is 20 cm. It consists of 5 cm carbon armor (in the backup design), 1 cm first wall, 12.5 cm bulk material, and 1.5 cm steel

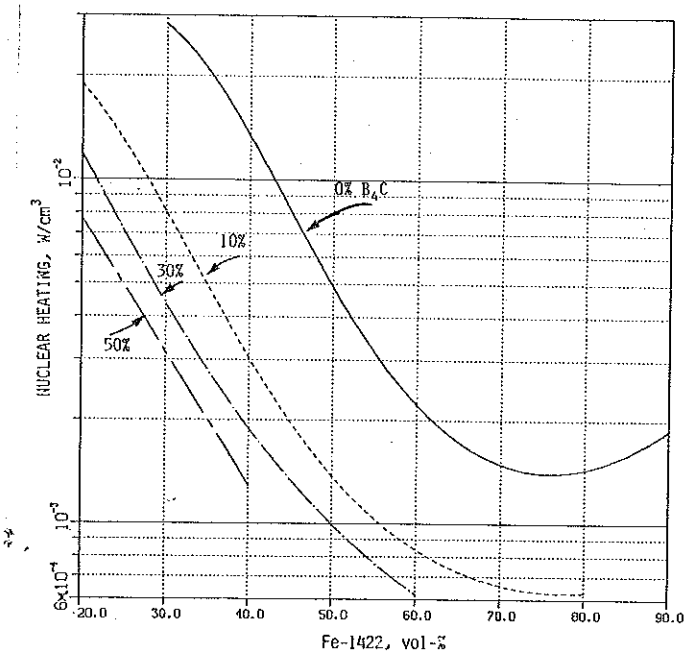

Fig. 3. Maximum nuclear heating in the TF case for 1.3 MW/m^2 neutron wall loading as a function of the Fe-1422 concentation in the inboard blanket and shield for different boron-carbide concentrations (balance is H_2O).

jacket for structure purposes. Type 316 stainless steel is used for the first part instead of Fe-1422. A 3-cm vacuum gap between the two parts is used to accommodate thermal expansion and engineering tolerance The second part is divided into seven layers: five layers of Fe-1422 with water coolant, each 9 cm thick; and two layers of B_4C with steel cladding material and water coolant, each 5 cm thick. The equivalent homogeneous compositon for the first and second part is the 80% Fe-1422, 10% B_4C, and 10% H_2O, as defined from the previous analysis. Two steel jackets are used for the second permanent part; each is 1.5 cm thick for structural purposes. The maximum values for the neutron fluence, copper-induced resistivity, and dpa after 6 $MW-y/m^2$ neutron expsosure were examined. These quantities are reduced for the heterogeneous shield. The neutron fluence and the dpa drop by 18% and 25%, respectively, in comparison with the homogeneous case. The dose in the insulators drops except for the case with boron carbide away from the magnet. In fact, the neutron dose drops while the gamma dose increases with a net decrease in the total dose. The drop in the neutron flux, which reduces the dose in the insulator materials, is caused by the use of more Fe-1422 in the high energy region of the neutron flux where iron is more effective in slowing down the neutrons through inelastic scattering, the use of more B_4C in the low energy region of the neutron flux to benefit from the elastic scattering of the light materials (C, B, H, O), and the high absorption cross section of the low energy neutrons in ^{10}B.

The reference design for the inboard blanket and bulk shield evolving from the previous analysis is listed in Table 2. Type 316 stainless steel is utilized for the first wall and portion of the inboard blanket and shield integrated with the torus sector module. The rest of the inboard blanket and shield employs Fe-1422 and B_4C materials. Fe-1422 has the advantage of low nickel and chromium content as compared to the other steel types (Types 316 and 304) which result in less long-term radioactivity. The boron carbide is used with a density factor of 0.9

Table 2. Inboard Blanket and Shield Design

Zone Description	Zone Thickness (cm)	Zone Composition Percentage by Volume
First wall armor[a]	5.0	100% C
First wall	1.0	50% 316 SS, 50% H_2O
Blanket & shield (A)	12.5	90% 316 SS, 10% H_2O
Jacket	1.5	100% 316 SS
Vacuum gap	3.0	Vacuum
Jacket	1.5	100% Fe-1422
Blanket & shield (B)	45.0	90% Fe-1422, 10% H_2O
Blanket & shield (C)	10.0	72% B_4C (0.9 D.F.) 18% Fe-1422
Jacket	1.5	100% Fe-1422

[a]Carbon is used only in the backup design.

to reduce the fabrication cost by avoiding the need for thermal sintering process.

Table 3 gives the radiation response parameters in the inboard portion of the TF coils. The maximum neutron fluence is below the reported damage threshold for the Nb_3Sn conductor by a factor of 2.5. The maximum induced resistivity in the copper stabilizer is 3.1×10^{-8} Ω-cm and it drops very fast with respect to the depth in the TF coils. The maximum dose in the thermal insulator is 1.6×10^9 rad, which is well below the acceptable limit. The maximum nuclear heating in the superconductor is 9×10^{-5} which does not cause any design difficulty for the TF coils.

The analysis given in this section is based on the use of carbon armor for the protection of the inboard first wall. However, the current reference design has a stainless steel armor instead of the carbon which increases the available radial thickness for the inboard shielding by ~3.9 cm. This change improves the shielding performance and increases the magnet protection.

Outboard Shield

In addition to radiaton protection of reactor components, the design of the outboard shield is critical in satisfying the personnel access requirements. The biological dose rate in the reactor building outside the bulk shield should be $\lesssim$2.5 mrem/h within 24 h after shutdown with all shield in place. Since decay gamma rays typically have a short mean-free path in moderately heavy materials, the contribution to the biological dose for a person in the reactor building comes essentially from the 5-15 cm of materials located at the outermost region of components located in the reactor building. Therefore, satisfying the personnel access criterion requires that (a) the bulk and penetration shields be effective in significantly reducing the neutron flux at the exterior components; and (b) materials in the outermost region of the exterior components (including the outer region of the bulk and penetration shields) do not produce strong decay gamma rays. Fe-1422, B_4C, and H_2O constitute a good material composition for the outer bulk shield. In addition, a small amount of lead in the outer region is beneficial as it attenuates the decay gammas from the inner region. Lead does not produce significant long-term activation products.

The radial thickness of the outboard shield in the initial analysis is 0.9 m behind a 0.5 m tritium-producing blanket. An optimization process was carried out to define a suitable composition using Fe-1422, B_4C, and H_2O material in a homogeneous model at the reactor midplane. The results were used as input for a heterogenous analysis similar to the procedure used for the inboard blanket and shield.

Table 3. Radiation Response Parameters in the Inboard Portion of the Toroidal Field Coils Based on 1.3 MW/m^2 Neutron Wall Loading and 6 $MW\text{-}y/m^2$ Neutron Exposure

Minimum neutron fluence in the superconductor, E > 0.1 MW (n/cm^2)	3.88×10^{17}
Maximum induced resistivity in the copper stabilizer (Ω-cm)	3.10×10^{-8}
Maximum atomic displacement in the copper stabilizer (dpa)	2.54×10^{-4}
Maximum nuclear heating in the superconductor (W/cm^3)	
Neutron	0.92×10^{-5}
Gamma	8.24×10^{-5}
Total	9.16×10^{-5}
Nuclear heating in the superconductor and the TF case, and dewar (W/cm)	
Neutron	0.35
Gamma	6.86
Total	7.21
Nuclear heating in the superconductor and the TF case (W/cm)	
Neutron	0.62
Gamma	16.10
Total	16.72
Dose in the thermal insulator (rads)	
Neutron	1.6×10^9
Gamma	0.9×10^9
Total	2.5×10^9

A comprehensive analysis was performed to minimize the energy leakage and the average neutron energy leaking from the outboard shield. The neutron energy leakage was taken as a good measure of both the neutron flux intensity and the shift in the neutron spectrum. Softening the neutron spectrum is necessary to reduce the producton rate of long-lived isotopes which are generated mainly by high-energy reactions such as (n,2n) and (n,p). A homogeneous model was used to define the shield composition in the 90 cm outboard shield thickness. The calculations were performed for a wide range of compositions similar to those used for the inboard blanket and shield. Fe-1422 and H_2O volume fractions were varied from 0.1 to 0.9 with four different B_4C volume fractions: 0, 0.1, 0.3, and 0.5 with the balance as H_2O. As an example of the results, Fig. 4, gives the total energy leakage per fusion neutron from the outboard shield as a function of the Fe-1422 concentration for four different B_4C concentrations. The minimum energy leakage occurs with a composition of 80% Fe-1422, 10% B_4C, 10% H_2O, while the neutron energy leakage is 0.18 eV/DTn. The neutron energy leakage shows a small difference between the lowest values of 0 and 10% B_4C concentration in the shield although the difference in the gamma energy leakage is a factor of 4 more for 0% B_4C concentration. The reference outboard shield design shown in Table 4 was based on a heterogeneous analysis similar in nature to that described earlier.

Penetration Shield

In order to perform the penetration shield analysis for the neutral beam (NB) injectors and the divertor system for the INTOR design, elaborate calculations were carried out in great detail to assess the impact on the reactor operation and accessibility after shutdown. A three-dimensional model describing the details of the reactor system was used in the analysis. The general-purpose Monte Carlo code MCNP[2] was used for the calculations with a continuous energy representation for the nuclear cross sections. The energy spectrum and the spatial distribution of the

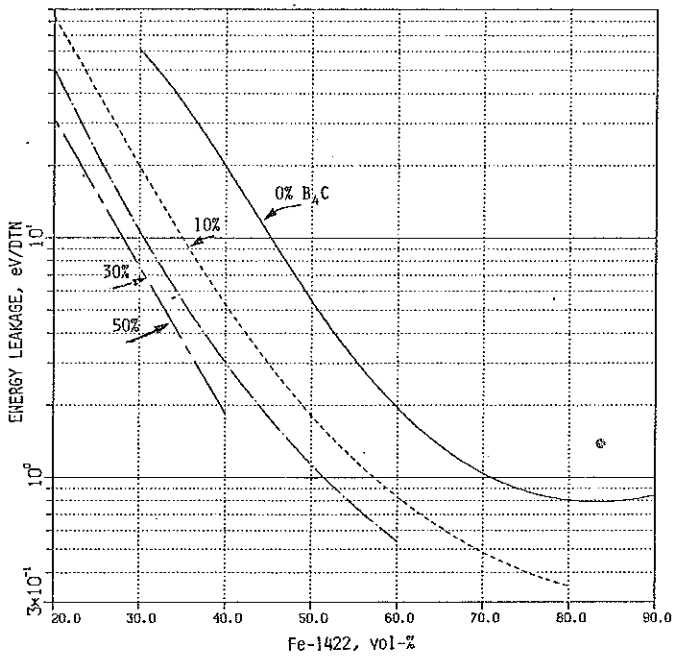

Fig. 4. Energy leakage per fusion neutron from the outboard shield as a function of the Fe-1422 concentration in the outboard shield for different boron carbide concentrations (balance is H_2O).

Table 4. Outboard Shield Design

Zone Description	Zone Thickness (cm)	Zone Composition Percentage by Volume	
Shield jacket	1.5	100%	Fe-1422
Fe-1422 shield	63.0	99%	Fe-1422
		1%	H_2O
B_4C shield	30.0	32.5%	H_2O
		45.0%	Fe-1422
		12.5%	B_4C
		10.01%	void
Shield jacket	1.5	100%	Fe-1422
Pb shield	4.0	100%	Pb

personnel access requirements of $\leq$2.5 mrem/h after shutdown. D-T source neutrons were considered in the analysis. Coupled neutron and neutron-induced photon transport during the operation and decay photon transport after shutdown using the same geometrical model were performed.

The three-dimensional geometrical model, shown in Fig. 5, describes the whole reactor where the different reactor components are presented explicitly in the model. The model makes use of the reactor symmetry (12 toroidal field coils, 6 neutral beam injectors, 12 divertor ducts) by considering a 30-deg sector. This sector includes one TF coil, one divertor duct, and one-half NB injector as shown in Fig. 5.

Continuous energy representation for the nuclear cross section (pointwise data) was used for the transport calculation. All the nuclear cross sections were generated from ENDF/B-IV data files except for manganese and molybdenum. The nuclear cross sections for these two elements were generated from ENDL data files. The neutron and photon energy ranges were 2.2 $\times 10^{-8}$ to 15 MeV and 0.01 to 15 MeV, respectively, for the calculation.

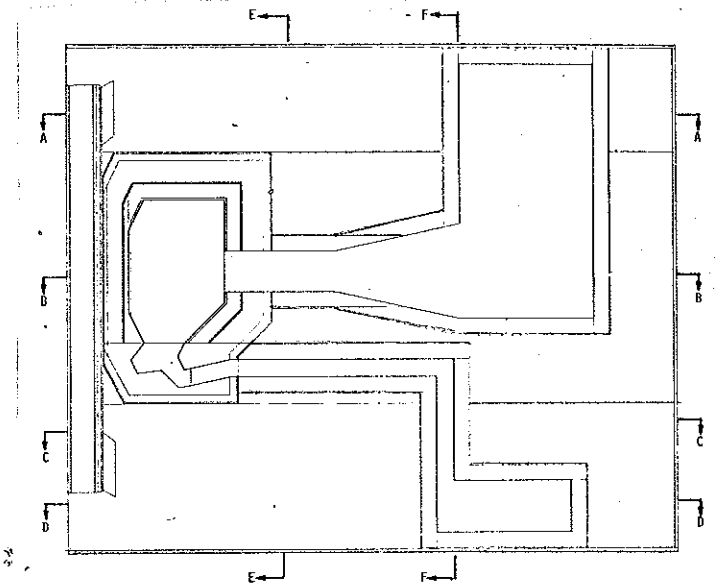

Fig. 5. Vertical cross section of the 3-D geometrical model used for the shielding analysis between the toroidal field coils showing the blanket, shield, neutral beam, divertor, and part of TF coil.

The neutron and neutron-induced photon transport calculations were performed with the MCNP code (a general Monte Carlo Code for neutron and photon transport). Three variance reduction schemes were employed for the calculations; these are splitting, Russian roulette, and weight cutoff with Russian roulette. Neutron fluxes and nuclear heating rates averaged over segmented zones and surfaces were calculated for the different reactor components.

The nuclear heating in the neutral beam box shows a maximum of 23 $\times 10^{-3}$ W/cm^3 in the area facing the plasma and a minimum of 0.6 $\times 10^{-3}$ W/cm^3 in the upper right corner.

In order to satisfy the 2.5 mrem/h dose limit on the outer surface of the shield after 24 h from shutdown, a three-dimensional dose analysis was performed. The neutron fluxes from the three-dimensional neutron transport calculation were used to generate a gamma source at 24 h after shutdown in every reactor zone. Using this gamma source, a gamma transport calculation was carried out for the same geometrical model to obtain the gamma flux, gamma heating, and radiation exposure dose in several locations in the reactor.

The results show the following shield thicknesses required to achieve an exposure dose in the reactor building of $\leq$2.5 mrem/h within 24 h from shutdown: (a) 100 cm for the neutral beam drift tubes; (b) 75 cm on the surfaces of the beam injector box facing the drift tubes; and (c) 50 cm for the rest of the neutral beam system and the divertor ducts.

References

1. Y. Gohar, M. A. Abdou, and J. Jung, Chapt. X, "Radiation Shielding," INTOR/NUC/81-10, The U.S. INTOR Contribution to the International Tokamak Reactor Phase-I Workshop, Conceptual Design, US INTOR/81-1 (June 1981).
2. LASL GROUP X-6, "MCNP-A General Monte Carlo Code for Neutron and Photon Transport," Los Alamos National Laboratory Rep. LA-7396-M (1979-Rev.).